Original Article

Shape Optimization of Retainer Design for Maxillary Anterior Resin-Bonded Fixed Partial Dentures

Yung-Chung Chen, DDS, MDsc, PhD
Department of Stomatology,
Division of Prosthodontics, National Cheng Kung University Hospital,
College of Medicine, National Cheng Kung University, Tainan, Taiwan
Institute of Oral Medicine,
College of Medicine, National Cheng Kung University, Tainan, Taiwan

Yuan-Ray Chang, MS
Department of Mechanical Engineering,
National Cheng Kung University,
Tainan, Taiwan

Chi-Lun Lin, MS, PhD
Department of Mechanical Engineering,
National Cheng Kung University,
Tainan, Taiwan

Corresponding author:
Chi-Lun Lin, MS, PhD
Assistant Professor, Department of Mechanical Engineering, National Cheng Kung University, Tainan, Taiwan R.O.C.
Tel: +886-6-2757575 ext. 62190
E-mail: linc@mail.ncku.edu.tw

Abstract

Objective

Given the unfavorable survival rates reported in previous studies, the improvement of resin-bonded fixed partial dentures (RBFPDs) is unquestionably necessary. Clinically, most failures of RBFPDs are attributed to interfacial debonding and inadequate retainer design. This paper presents an automated optimization approach that utilizes the framework of finite element analysis to obtain retainer designs for RBFPDs that can reduce the risk of debonding and further extend clinical service time.

Material and methods

The automated optimization process was developed and performed to determine the optimal RBFPD retainer designs in an iterative manner. The overall optimization process consisted of two steps: the manual building of models and the automated optimization process itself. Ten specimens for each group, the traditional group and optimal group, were fabricated for each design. The specimens were then loaded to failure in order to compare their mechanical performance.

Results

The in vitro mechanical tests indicated that the optimal design obtained was not able to outperform the traditional design. It was found that the assigned values simulating the adhesive's bonding strengths were set too high in the automated scripts. By lowering the adhesive's bonding strengths to reasonable values in the second set, the performance of the optimal design was experimentally validated. The optimal design outperformed the traditional design in terms of the amount of tooth preparation and debonding area. In the validation experiment, the optimal design was found to have a higher peak force and first load drop than the traditional design did.

Conclusion

The experimental results validated the automated optimization process and suggested that it can be used to generate optimized designs for various clinical conditions and to provide scientifically sound preparation guidelines for clinicians.

Key words: automated modeling, finite element analysis, resin-bonded fixed partial dentures, shape optimization

Introduction

During the past few decades, minimally invasive treatment protocols have become popular due to the development and improvement of dental adhesive materials, and hence, the philosophy for designing dental prostheses has also changed. When a patient needs a prosthetic restoration for missing anterior teeth, the fundamental rule is to restore function and esthetics at minimal biological cost[1]. Resin-bonded fixed partial dentures (RBFPDs), which are recognized as constituting a minimally invasive treatment, were first introduced by Ibsen[2] and Rochette[3]. The concept underlying their development and use was to decrease the amount of teeth preparation and to preserve healthy tooth tissue as much as possible[4].

RBFPDs can be made with different material systems. In early designs, metal alloys were used in the fabrication of the dental bridges. Recently, fiber-reinforced composites (FRCs) and ceramic materials have been increasingly adopted in fabricating RBFPDs due to the growing esthetic demands of patients. However, the application of ceramic materials is significantly limited because their brittleness leads to more tooth tissue removal[5, 6]. Consequently, FRC systems have drawn increasing attention for use in RBFPDs because they can provide a tooth-colored appearance and retain the advantages of minimal invasion. Moreover, FRC FPDs can be fabricated directly in a patient's mouth or indirectly by a dental technician. If slight damage to an FRC FPD occurs while the patient is wearing it, the denture can be restored directly in the patient's mouth[7]. Hence, FRC FPDs can provide better convenience than metal and ceramic FPDs. In addition, the lower cost of FRC FPDs makes them a more affordable option for patients. However, there are also some disadvantages to FRC FPDs. The strength of FRC is inferior to the strength of metal and ceramic, and the surfaces of FRC can become worn more easily and accumulate more plaque[8, 9].

For the main scope of the present study, the authors reviewed the success rates of FRC FPDs with thin wing-shaped retainers only. An FRC FPD was defined as successful if it exhibited or resulted in no pontic fracture, glass fiber fracture, abutment tooth fracture, chipping of the composite resin, or retainer debonding when worn. Frese and his colleagues reported a 72.6% success rate for anterior FRC FPDs at 54 months[10], while Malmstrom and her colleagues reported that 89.4% of anterior FRC FPDs that were all fabricated directly in patients' mouths remained successful at two years[11]. Spinas and his colleagues reported a 93.8% success rate for anterior FRC FPDs given to teenage patients after five years of observation[12], while Kumbuloglu and her colleagues also observed a relatively high success rate of 92.6% for anterior FRC FPDs at 58 months[13]. However, lower success rates for anterior FRC FPDs have also been noted. For example, Heumen and his colleagues reported that only 45% of anterior FRC FPDs survived at 5 years[7], and Wolff and his colleagues reported an overall survival rate of 53.0% and a functional survival rate of 73.5% for FRC FPDs over the 48-month observation period of a clinical trial that they conducted[14].

According to the aforementioned studies, the most common failure mode of FRC FPDs is chipping of the composite resin, followed by debonding of the retainer and fracture of the glass fiber. As such, FRC FPDs can be viewed as a feasible short-term to medium-term treatment option, but there is still much room for improvement in terms of their success rate. Relatedly, research supporting the long-term usage of FRC FPDs is currently lacking[15], but the long-term success rate for such dentures is certainly expected to be lower than the short-term and medium-term success rates.

At present, the traditional way to design FPD retainers is to create a covering area for bonding on the lingual surface of a tooth that is as large as possible[16, 17]. The most common way to test the mechanical performance of an FRC FPD is to use a universal testing machine to apply load to the FRC FPD until it fractures. However, there are many drawbacks to this load-to-fracture method, such as the expensive material costs, time-consuming specimen preparation, and difficulties in controlling specimen dimensions. Furthermore, the associated experimental results do not allow for a straightforward determination of how any new FPDs should be designed. Therefore, a number of studies have utilized the finite element method and observed the stress distribution in FPD structures in order to effectively optimize FRC FPD designs[18-21]. However, while this approach is very convenient for comparing stress distributions among different designs, it is still a very time-consuming approach to use when modifying designs repeatedly. Moreover, it is difficult to determine when an optimal design has been achieved with this approach.

After a comprehensive literature review, we found that the consideration of biomechanical issues during the clinical design process used for anterior cantilever FRC FPDs is insufficient. To reduce the risk of a retainer debonding, its optimal shape for minimizing interfacial stresses should be determined. Therefore, the present study was aimed at developing an automated optimization process that utilizes the framework of finite element analysis to solve the debonding problem and increase the success rate of anterior cantilever FRC FPDs.

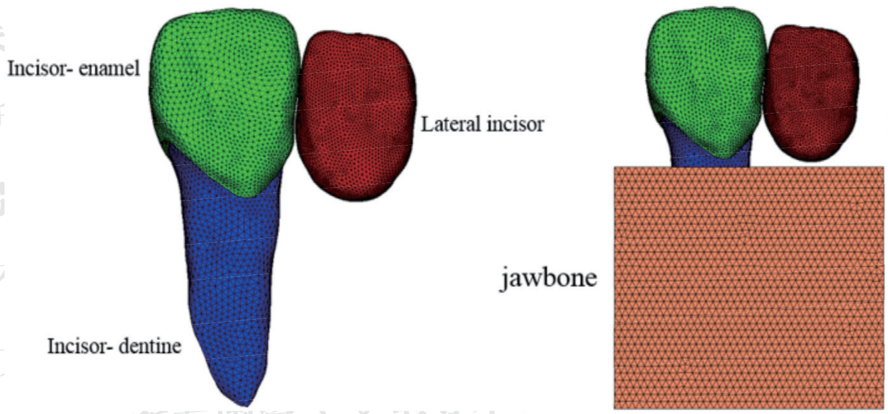

Fig. 1. The geometric parts of the finite element mode

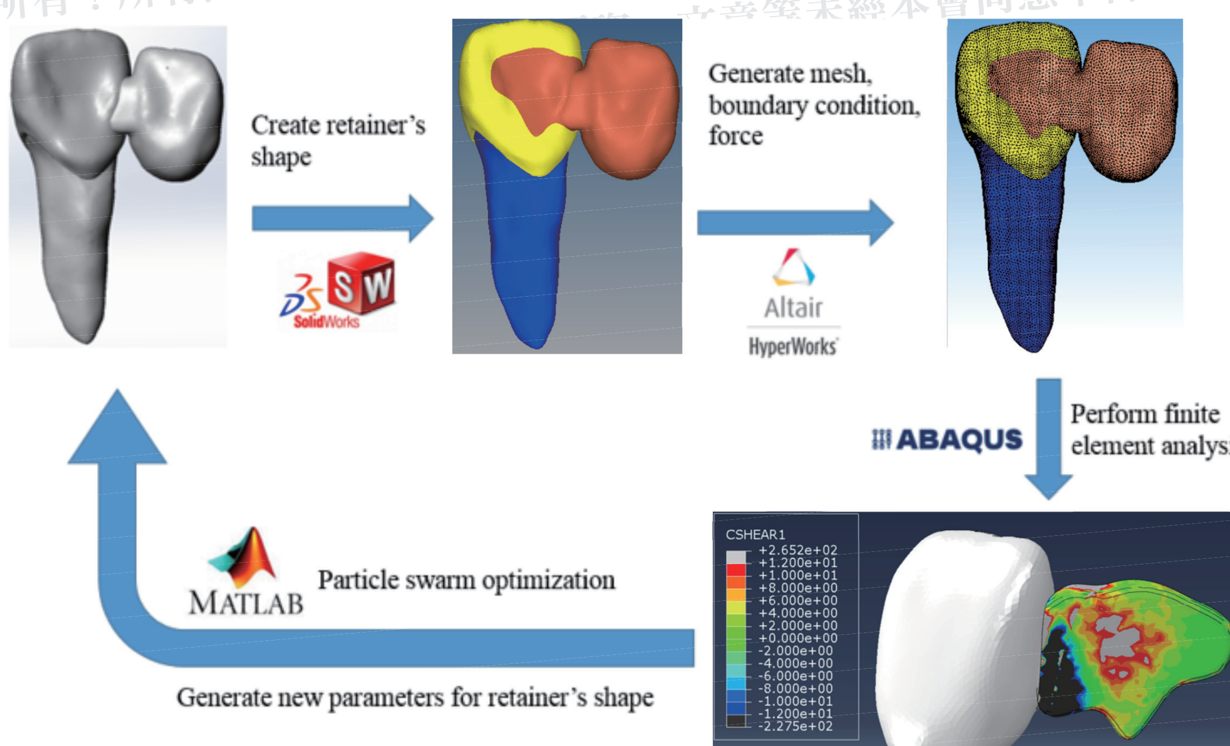

Fig. 2. The automated optimization process

Material and methods

To attain the optimal designs for anterior cantilever FRC FPDs, a numerical optimization process and in vitro experiment for validation were included in the present study. The study focused on replacing a missing maxillary lateral incisor with an RBFPD, and the retainer was designed to be bonded to a central incisor. The overall optimization process consisted of two steps: the manual building of models and the automated optimization process itself. The physical model of a central incisor and the cantilevered pontic was manually constructed using the software SolidWorks (Solidworks 2018, Dassault Systèmes SolidWorks Corporation, MA, United States).

Numerical optimization process

In this study, the geometric models used contained a central incisor, a cantilevered pontic for the lateral incisor, and a rectangular bone block (see Fig. 1). Both incisors' contours were obtained from real teeth scanned by a micro-CT scanner (Skyscan 1076, Bruker, Belgium). The material sections of the incisor model including enamel, dentine, and pulp were segmented.

The automated optimization process was conducted as follows. First, the shape of the retainer shape was devised using the software SolidWorks. Second, meshes of great quality were generated using the software Hypermesh (Hyperworks, Altair, MI, United States). The element sizes were 0.2 mm

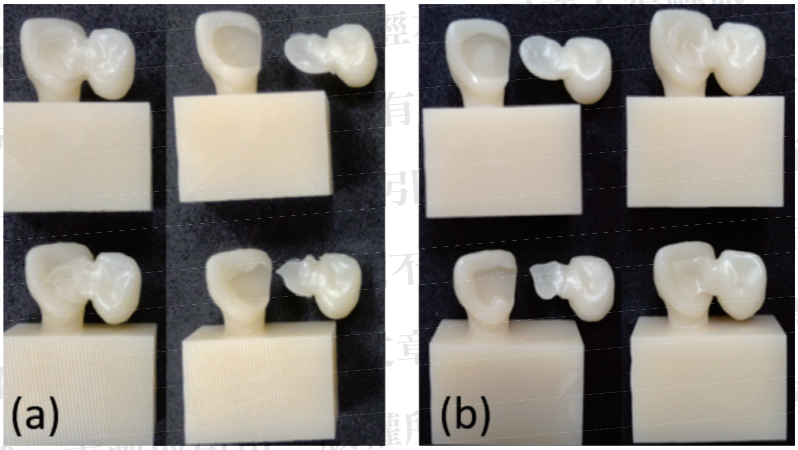

Fig. 3. Specimens of traditional and optimized designs: (a) 1st set (b) 2nd set


Fig. 4. The configuration of in vitro mechanical test

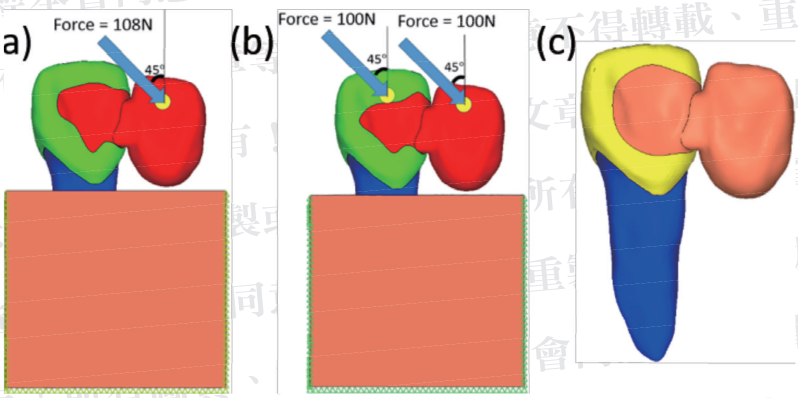

Fig. 5. The optimization results of the realistic RBFPD retainer: (a) Optimal design for the first loading type,; (b) optimal design for the second loading type,; (c) traditional design

for the RBFPD and the incisor and 0.2 ~ 0.8 mm for the bone block. Using ABAQUS element type C3D4, about 400,000 elements and 80,000 nodes were generated over the entire model. Next, a distributed load was applied at the lingual surface of the pontic of the RBFPD, and both sides of the bone block were fixed as the boundary condition. Two types of loading situation were simulated, including applying a load of 108N at the pontic only and applying a load of 100N at both the central incisor and pontic. Third, the finite element model was solved by using the software ABAQUS (ABAQUS 14-2, Dassault Systèmes SolidWorks Corporation, MA, United States) to retrieve the stresses at the interface between the RBFPD and central incisor. Last, the tensile stress and shear stress values at the interface between the retainer and prepared tooth were collected. The areas with higher stresses than the assumed adhesive's bonding strength were summed up as the total debonding area. The particle swarm optimization (PSO) algorithm was implemented to minimize the total debonding area. This study used ten vectors as the design variables to describe the shape of the retainer. The initial design (defined as the traditional design) was designed according to current clinical practices, in which the retainer is designed to cover the lingual side of the tooth as much as possible in order to maximize the contact area, as shown in Fig. 5(c). In each iteration, the PSO algorithm generated new design variables for the retainer's shape and automatically repeated the aforementioned steps until reaching convergence. The maximum number of iterations was set at 30. The whole process is shown in Fig. 2. Finally, the mechanical performance of the optimal design was compared with that of the traditional design.

In vitro experiment for validation

To ensure that the optimal design obtained from the numerical optimization process was valid,

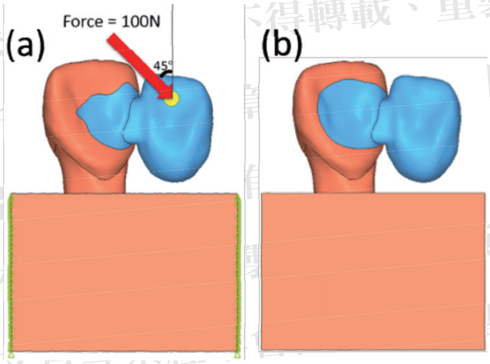

Fig. 6. The optimization results of the simplified RBFPD retainer for the first set of validation: (a) optimal design,; (b) traditional design

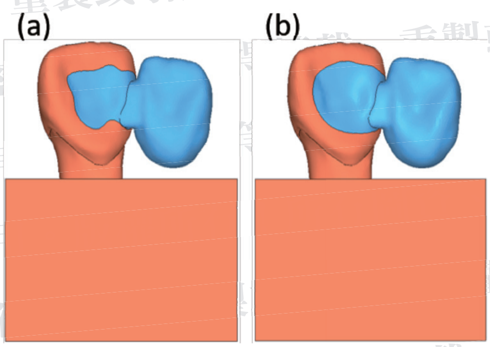

Fig. 8. The optimization results of the simplified RBFPD retainer for the second set of validation: (a) optimal design,; (b) traditional design

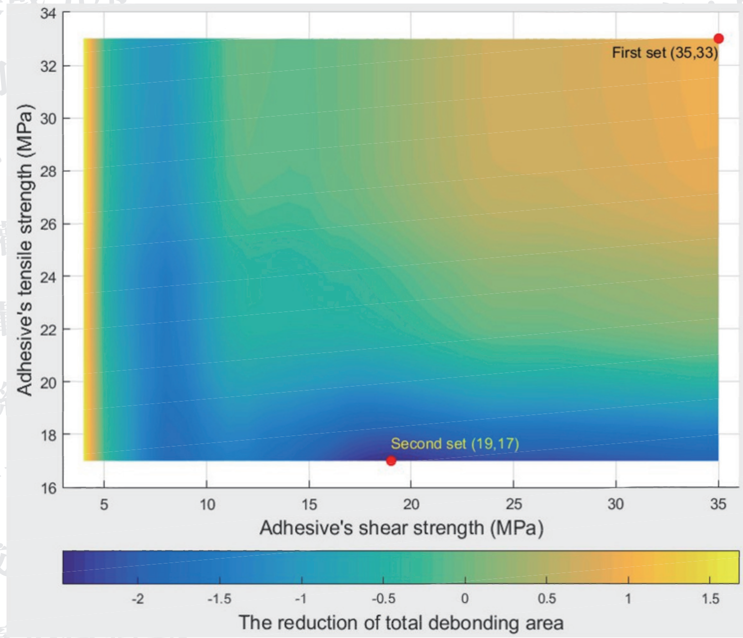

Fig. 7. The comparison of traditional and optimal designs in different adhesive's bonding

a simplified model was used to determine the optimal design so that the same settings could be exactly duplicated in both the finite element simulation and the experiment. The mechanical performance of the traditional and optimized designs was then compared.

In the experiment, the entire model and the RBFPDs were made of PMMA (see Fig. 3). Ten specimens were fabricated for each design. The fabricated traditional and optimized RBFPDs were adhered to the central incisor using resin cement (RelyX U200, 3M ESPE, MN, United States). Both sides of the rectangular PMMA block were clamped by a fixture. In addition, an acoustic emission sensor was glued onto the rectangular PMMA block to monitor the development of cracks in the specimens during loading. A universal testing machine (JSV-H1000, Japan Instrumentation system, Narashi, Japan) was used to apply a compressive load to the pontic of the given RBFPD. The force was applied at 2 mm below the incisal edge using a steel ball indenter with a diameter of 2 mm and a constant loading speed of one millimeter per minute. The load was applied until the RBFPD debonded from the central incisor. The configuration of the experiment is shown in Fig. 4.

Results

The first part of the results presented here are the results of the numerical optimization process. A more realistic RBFPD design was simulated along with the automated optimization process under two loading conditions. The second part of the results presented here are the results for the validation of the numerical optimization process, in which a simplified RBFPD design was optimized and its results were compared with those of an in vitro mechanical experiment.

1. Deriving designs of RBFPDs for two loading conditions

As previously mentioned, the retainer designs under two types of loading situations, that is, loading at the pontic only or loading at both incisors, were simulated iteratively for optimization. The optimal designs for the first and the second loading types are shown in Figs. 5a and 5b. The traditional design is shown in Fig. 5c. The debonding areas and tooth preparation amounts were compared and are listed in Table 1. The debonding area of the RBFPD was found to be smaller when the load was applied at the enamel rather than at the retainer. It was further found that both optimal designs required lower tooth preparation amounts than the traditional

Table 1. Comparison of traditional and optimal designs for realistic RBFPD retainer

	Loads at central incisor and pontic (100N each)		Load only at pontic (108N)	
	Traditional	Optimal	Traditional	Optimal
Debonding area (mm^2)	15.69	10.97	12.26	10.63
Preparation amount (mm^3)	37.18	26.44	37.18	30.25

Table 2. First set - comparison of traditional and optimal designs for validation

	Debonding area (mm^2)	Preparation amount (mm^3)
Traditional	2.99	36.64
Optimized	2.07	26.04

Table 3. First set – in vitro mechanical test results for the traditional design

	Peak force	Slope	Number of AE events
T1	116.4	62.35	25
T2	47.8	45.8	83
T3	77.7	52.86	15
T4	122.7	55.28	23
T5	83.4	44.7	127
T6	51.6	42.5	39
T7	158.3	55.37	43
T8	107.4	44.82	44
T9	133.3	47.85	26
T10	114.5	41.27	15
Average	101.31	49.28	44
SD	33.73	6.49	33.53

Table 4. First set – in vitro mechanical test results for the optimal design

	Peak force	Slope	Number of AE events
O1	52.4	46.83	85
O2	43.3	30.15	5
O3	28.8	29.72	9
O4	66	46.3	13
O5	53.9	41.06	28
O6	61.3	39.19	16
O7	25.3	24.7	4
O8	59	44.03	13
O9	61.1	41.8	29
O10	28	34.19	64
Average	47.91	37.8	26.6
SD	14.68	7.28	25.66

design and that the debonding areas for both optimized designs were smaller.

2. Validation of the optimization process

2.1. Optimization process (1st set)

A distribution load of 100N was applied at the pontic, and both sides of the cuboid were fixed (see Fig. 6a). The bonding strengths, 33 MPa for tensile strength and 35 MPa for shear strength, were assumed to be the same as for the enamel bonded to the adhesive. The optimal design and the traditional design are shown in Figs. 6a and 6b, respectively. Compared to the traditional design, the optimal design had better performance in terms of both the amount of tooth preparation and the total debonding area (see Table 2).

2.2. In vitro validation (1st set)

After indentation, the force-displacement curve and AE signal were obtained. Nineteen specimens were debonded and only one specimen was fractured at the connector. The peak force, slope of the force-displacement curve, and number of AE events for the traditional and optimal designs are shown in Table 3 and Table 4, respectively. The traditional designs had higher peak forces, slopes, and numbers of AE events than the optimal designs did. This sug-

Table 5. Second set - comparison of traditional and optimal designs for validation

	Debonding area (mm^2)	Preparation amount (mm^3)
Traditional	7.92	36.64
Optimized	6.36	27.87

Table 6. Second set - in vitro mechanical test results for the traditional design

	Peak force	First force drop	Number of force drops	Number of AE events
T1	13.63	13.14	46	80
T2	20.50	11.38	43	86
T3	28.05	12.65	85	210
T4	21.28	11.67	55	202
T5	10.49	8.53	66	210
T6	36.58	13.04	28	81
T7	32.17	27.85	39	138
T8	19.42	19.42	68	185
T9	25.30	14.02	28	72
T10	22.16	13.24	43	82
Average	22.96	14.49	50.1	134.6
SD	7.52	5.15	17.42	57.76

gests that the traditional designs outperformed the optimal ones.

Thus, the optimal design obtained was shown to have poorer performance in the experiment. This poorer performance was most likely caused by the settings of the adhesive's bonding strengths being wrong. The bonding strengths were set as 35 and 33 MPa for shear stress and tensile stress, respectively. However, according to the literature, the ranges of bonding strengths for shear stress and tensile stress are 4-35 and 17-33 MPa, respectively. Hence, the debonding areas of the traditional and optimal designs were reevaluated with different bonding strengths for the adhesive. The resulting comparison of the total debonding area of the traditional and optimal designs for the different adhesive bonding strengths is shown in Fig. 7. The cases in which the optimal design had a lower total debonding area were marked with a triangular sign, while the cases in which the traditional design had a lower total debonding area were marked with a circular sign. If the bonding strengths between the adhesive and the PMMA were actually located at the region of the circular sign, then it would make sense that the traditional design was better than the optimal design.

2.3. Optimization process (2nd set)

The finite element simulation of the second set was the same as that for the first set. The only difference was in the adhesive's bonding strengths. Specifically, strengths of 19 and 17 MPa for the shear stress and tensile stress, respectively, were assumed. Based on the evaluation of the parametrical study shown in Fig. 7, this selected configuration of bonding strengths would produce the largest discrepancy in the total debonding area between the traditional design and optimal design.

The resulting optimal design and the traditional design are shown in Figs. 8a and 8b, respectively. Compared to the traditional design, the optimal

Table 7. Second set - in vitro mechanical test results for the optimal design

	Peak force	First force drop	Number of force drops	Number of AE events
O1	54.03	15.00	9	102
O2	56.00	21.08	13	76
O3	34.03	24.91	31	146
O4	32.26	13.14	14	75
O5	36.58	16.28	12	53
O6	39.91	12.65	10	54
O7	44.52	19.02	10	46
O8	61.49	20.79	11	44
O9	10.40	10.40	71	177
O10	53.45	17.95	6	29
Average	42.27	17.12	18.7	80.2
SD	14.31	4.25	18.58	45.55

design had better performance in terms of both the amount of tooth preparation and the total debonding area (see Table 5).

2.4. In vitro validation (2nd set)

After indentation, the force-displacement curve and AE signal were obtained. All the models were debonded. The peak force, first force drop, number of force drops, and number of AE events of the traditional and optimal designs are shown in Table 6 and Table 7, respectively. All the optimal designs had higher peak forces and first force drops than the traditional designs, which suggested that the optimal designs outperformed the traditional ones. Thus, the optimization process was validated by the experiment performed with the adjusted adhesive bonding strengths.

Discussion

The optimal solution achieved a lower amount of tooth preparation and smaller debonding area at the same time. This result suggests that a larger retainer does not always provide better mechanical performance. Rather, the shape of the retainer plays a more important role in this regard. It was observed during the iteration process that the shape of the retainer tended to evolve to avoid the direct load, such that the load was finally applied on the enamel. Interestingly, this result matched the objective of current clinical practice.

Unexpected failure occurred in three of the twenty samples in the first set of the validation experiment. The O1 and O4 samples showed cracks and the connector of the T5 sample broke into two parts at a peak force of 83.4 N, which was much lower than the forces that the other samples with the traditional design were able to sustain. We suspected that the manufacturing process was not carefully performed so that local sharp edges were produced and concentrations of stress arose at these locations. Furthermore, two types of surface finish were observed among the twenty samples. As a result, one type of the samples had a smoother surface finish, while on the surface of the others a clear direction of lay was seen. A significant difference in the peak force between these two groups of samples was found in the experimental results (Tables 3 and 4). In order to obtain a more consistent sample condition for all the samples, the aforementioned issues were fixed by communicating with the dental technician before manufacturing the samples for the second validation experiment.

Previous studies have reported that the values of the tensile and shear strengths for an adhesive are distributed in wide ranges of 17-33 MPa and 4-35 MPa, respectively. The optimal design obtained in the first set of optimization was compared with the traditional design in the finite element simulations using all combinations of the strength values in the ranges. Fig. 7 shows the results of this parametric study as a contour plot, where the reduction of the total debonding area was the improvement achieved by the optimization. Thus, the colors with positive values indicate that the optimal design outperformed the traditional design. The contour plot suggested that the current optimal design would outperform the traditional design to a greater degree when both the tensile and shear strengths of the adhesive are higher. However, the validation experiment obtained an opposite result, which proved that the bonding strengths of the adhesive selected in the optimization process were too optimistic. According to the contour plot, the traditional design would be most likely to outperform the optimal design when the tensile and shear strengths were set as 17 and 19 MPa, respectively (i.e., the poorest optimal design with the most negative reduction of total debonding area). Thus, this configuration was selected to conduct the second set of optimization and the validation experiment, and the results did prove that our guess was correct.

The design variables considered in this research consisted of ten length vectors that defined ten points to form the outline of the retainer. The retainer contacted the tooth at a plane, but in practice, it can have a curved surface or other 3D shapes. In addition, other types of designs have been used in other research studies, such as designs featuring holes and ditches, in order to enhance the bonding strength at the interface[29, 33, 34, 52-54]. For future improvements, more design variables can be included in the optimization process to consider more types of retainer designs.

With regard to the patient-specific modeling, the shape of the teeth for a given patient can be parameterized. That is, measurements of different patients' teeth can be performed to define proper geometric parameters. The approach of using many vectors to define the retainer can also be applied to define a given tooth.

Conclusion

In this study, an automated optimization process was developed and performed to determine the optimal RBFPD retainer designs under different load conditions. However, the optimal design obtained was shown to have poorer performance than the traditional design in the first round of the validation experiment. It was found that the adhesive's bonding strengths were set too high. By lowering the adhesive's bonding strengths to reasonable values in the second set, the obtained optimal design was successfully validated, as the optimal design outperformed the traditional design in terms of the amount of tooth preparation and the debonding area. In the validation experiment, the optimal design had a higher peak force and first force drop than the traditional design did. The results of the experiment suggested that the automated optimization process can be used to generate optimal designs for various clinical conditions and to provide scientifically sound preparation guidelines for clinicians.

References

1. Edelhoff D, Sorensen JA. Tooth structure removal associated with various preparation designs for anterior teeth. J Prosthet Dent 2002;87:503-9.
2. Ibsen RL. Fixed prosthetics with a natural crown pontic using an adhesive composite. Case history. J South Calif Dent Assoc 1973;41:100-2.
3. Rochette AL. Attachment of a splint to enamel of lower anterior teeth. J Prosthet Dent 1973;30:418-23.
4. Murdoch-Kinch CA, McLean ME. Minimally invasive dentistry. J Am Dent Assoc 2003;134:87-95.
5. P P, P R, G G, W G. All-ceramic resin-boned bridges. A 3-dimensional finite-element analysis study. European Journal of Oral Sciences 1996;104:390-5.
6. C K, M R, M B, R L, G H. In vitro examination of the fracture strength of 3 different fiber-reinforced composite and 1 all-ceramic posterior inlay fixed partial denture systems. Journal of Prosthodontics 2002;11:248-53.
7. van Heumen CCM, van Dijken JWV, Tanner J, Pikaar R, Lassila LVJ, Creugers NHJ, et al. Five-year survival of 3-unit fiber-reinforced composite fixed partial dentures in the anterior area. Dent Mater 2009;25:820-7.
8. Behr M, Rosentritt M, Handel G. Fiber-reinforced composite crowns and FPDs: A clinical report. Int J Prosthodont 2003;16:239-43.
9. Bollen CML, Lambrechts P, Quirynen M. Comparison of surface roughness of oral hard materials to the threshold surface roughness for bacterial plaque retention: A review of the literature. Dent Mater 1997;13:258-69.
10. Frese C, Schiller P, Staehle HJ, Wolff D. Fiber-reinforced composite fixed dental prostheses in the anterior area: a 4.5-year follow-up. J Prosthet Dent 2014;112:143-9.
11. Malmstrom H, Dellanzo-Savu A, Xiao J, Feng C, Jabeen A, Romero M, et al. Success, clinical performance and patient satisfaction of direct fibre-reinforced composite fixed partial dentures - a two-year clinical study. J Oral Rehabil 2015;42:906-13.
12. Spinas E, Aresu M, Canargiu F. Prosthetic rehabilitation interventions in adolescents with fixed bridges: a 5-year observational study. Eur J Paediatr Dent 2013;14:59-62.
13. Kumbuloglu O, Ozcan M. Clinical survival of indirect, anterior 3-unit surface-retained fibre-reinforced composite fixed dental prosthesis: Up to 7.5-years follow-up. J Dent 2015;43:656-63.
14. Wolff D, Wohlrab T, Saure D, Krisam J, Frese C. Fiber-

reinforced composite fixed dental prostheses: A 4-year prospective clinical trial evaluating survival, quality, and effects on surrounding periodontal tissues. J Prosthet Dent 2017.

15. Ahmed KE, Li KY, Murray CA. Longevity of fiber-reinforced composite fixed partial dentures (FRC FPD) Systematic review. J Dent 2017;61:1-11.
16. Botelho M. Design principles for cantilevered resin-bonded fixed partial dentures. Quintessence Int 2000;31:613-9.
17. Stephen R, Martin L, Junhei F. Contemporary Fixed Prosthodontics. 2015:694-712.
18. Nakamura T, Ohyama T, Waki T, Kinuta S, Wakabayashi K, Takano N, et al. Finite element analysis of fiber-reinforced fixed partial dentures. Dent Mater J 2005;24:275-9.
19. Yokoyama D, Shinya A, Lassila LVJ, Gomi H, Nakasone Y, Vallittu PK, et al. Framework Design of an Anterior Fiber-Reinforced Hybrid Composite Fixed Partial Denture: A 3D Finite Element Study. Int J Prosthodont 2009;22:405-12.
20. Ootaki M, Shin-Ya A, Gomi H, Shin-Ya A, Nakasone Y. Optimum design for fixed partial dentures made of hybrid resin with glass fiber reinforcement by finite element analysis: Effect of vertical reinforced thickness on fiber frame. Dent Mater J 2007;26:280-9.
21. Magne P, Perakis N, Belser UC, Krejci I. Stress distribution of inlay-anchored adhesive fixed partial dentures: a finite element analysis of the influence of restorative materials and abutment preparation design. The Journal of prosthetic dentistry 2002;87:516-27.